analytical chemistry

pubs.acs.org/ac Article

High-Throughput Strategy for Glycine Oxidase Biosensor Development Reveals Glycine Release from Cultured Cells

Siba Moussa, Elena Rosini, Daryan Chitsaz, Loredano Pollegioni, Timothy E. Kennedy, and Janine Mauzeroll*

Cite This: *Anal. Chem.* 2021, 93, 16504−16511 Read Online

ACCESS | Metrics & More | Article Recommendations | Supporting Information

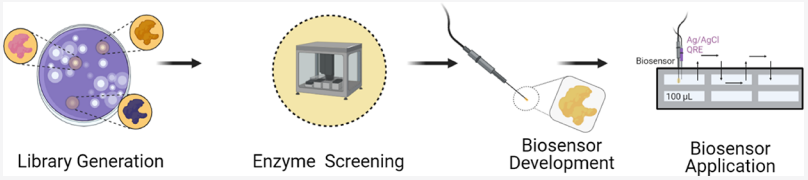

ABSTRACT: Glycine is an important biomarker in clinical analysis due to its involvement in multiple physiological processes. As such, the need for low-cost analytical tools for glycine detection is growing. As a neurotransmitter, glycine is involved in inhibitory and excitatory neurochemical transmission in the central nervous system. In this work, we present a 10 μM Pt-based electrochemical enzymatic biosensor based on the flavoenzyme glycine oxidase (GO) for localized real-time measurements of glycine. Among GO variants at position 244, the H244K variant with increased glycine turnover was selected to develop a functional biosensor. This biosensor relies on amperometric readouts and does not require additional redox mediators. The biosensor was characterized and applied for glycine detection from cells, mainly HEK 293 cells and primary rat astrocytes. We have identified an enzyme, GO H244K, with increased glycine turnover using mutagenesis but which can be developed into a functional biosensor. Noteworthy, a glycine release of 395.7 ± 123 μM from primary astrocytes was measured, which is ~fivefold higher than glycine release from HEK 293 cells (75.4 ± 3.91 μM) using the GO H244K biosensor.

INTRODUCTION

Biosensors are becoming increasingly popular for their ability to enable real-time analyte detection. The use of biosensors is revolutionizing many research areas, including neuroscience and clinical testing. Amperometric biosensors are one class of sensors that allow for quantification of concentration changes based on measured current changes.[1] One particular example of amperometric biosensors and their successful commercialization in point-of-care devices are glucose test strips.[2,3] Along the lines of amperometric biosensing, our laboratory has previously shown the success of amperometric enzymatic biosensors in pre-clinical studies on the detection of D-serine,[4,5] a co-agonist at excitatory NMDA receptors in the brain, especially at extrasynaptic sites.[6] A number of other enzymatic electrochemical probes have also been developed for neurotransmitter detection such as glutamate,[7,8] dopamine,[9] and acetylcholine.[10] No such amperometric sensors are available for localized measurements of the neurotransmitter and NMDAR co-agonist, glycine.

As a neurotransmitter, glycine is involved in inhibitory and excitatory neurochemical transmission in the central nervous system.[11] Glycine release in the brain has varying overall impact depending on the cellular release source.[12] It is endogenously synthesized from other amino acids, primarily in the liver and kidney, making it a non-essential amino acid.[13] Although non-essential, glycine plays other important roles in physiological functions of humans and animals. In the rest of the body, glycine has anti-inflammatory, cryoprotective, and immune modulating roles.[14] Previous efforts to associate glycine level measurement with diseased states have shown that low glycine levels are related to obesity, diabetes, and schizophrenia.[13] Nutritionally, insufficient glycine intake may result in suboptimal growth, impaired immune responses, and other adverse effects on health and nutrient metabolism.[15]

Currently, glycine levels are measured using chromatographic methods, which are expensive and time-consuming.[16−18] Glycine-detecting electrochemical sensors have been developed to avoid the shortcomings of chromatography.[16,19−21] However, none of these sensors have been developed for localized glycine measurements, making it impossible to measure glycine levels associated with synaptic transmission without microdialysis.[11,12]

Herein, we present a rapid approach for the development of an enzymatic amperometric electrochemical biosensor for time

Received: August 23, 2021
Accepted: November 16, 2021
Published: November 29, 2021

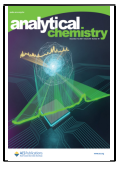

https://doi.org/10.1021/acs.analchem.1c03620
Anal. Chem. 2021, 93, 16504−16511

Scheme 1. Random Clone Selection Strategy and Schematic of High-Throughput Screening Methodology to Search for Variants with Enhanced Glycine Turnover Activity

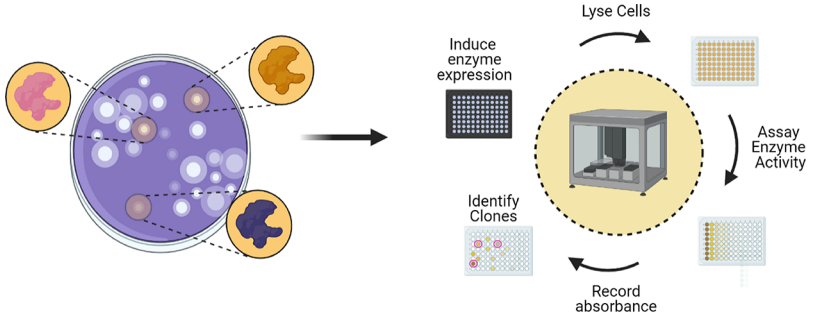

measurements of glycine release from localized regions. To develop the biosensor, we used high-throughput screening to identify glycine oxidase (GO) variants with increased glycine activity. In detail, we screened a library of GO clones produced through site-saturation mutagenesis at position 244 for enhanced activity on glycine (Schematic 1). GO is a flavoenzyme responsible for catalyzing the oxygen-dependent deamination of glycine in which hydrogen peroxide is produced as a side product.[22,23] The H244 residue on GO is localized in the active site cavity and is involved in optimization of the reaction catalyzed by GO.[24,25] Substitutions at the H244 position frequently result in a substrate turnover number increase compared to the wild-type GO.[24,26]

A selected recombinant GO variant (GO H244K) was used for enzymatic electrochemical biosensor development. First, the GO enzyme was immobilized on the electrochemical sensor surface. Next, GO turned over glycine into hydrogen peroxide (H_2O_2). The H_2O_2 diffused through a permselective polymer layer and was subsequently oxidized (0.5 V) on the electroactive sensor surface, where an oxidative current is measured that enables indirect glycine quantification.[4] To further reduce biosensor development time (~30%), an approach using high-throughput assay techniques was developed for biosensor calibration and application. We then measured glycine levels from astrocyte-conditioned media, HEK 293 cells, and primary astrocytes. Our biosensors were found to be useful in glycine detection measurements, making them an important new tool for localized glycine measurements in neurologically relevant systems (Scheme 1).

EXPERIMENTAL SECTION

Chemicals. Horseradish peroxidase (HRP), amino acids, ampicillin, chloramphenicol, and all other compounds were purchased from Sigma unless otherwise stated. The final concentration of ampicillin (Amp) and chloramphenicol (Cam) used were 100 and 34 μg/mL, respectively.

Library Generation and Variant Screening. A library of GO variants previously generated by site-saturation mutagenesis at position 244, using a QuikChange site-directed mutagenesis kit (Stratagene, La Jolla, CA), and the GO cDNA subcloned in the pT7(ΔBH)-HisGO plasmid were used for screening on glycine as a substrate.[26] The introduction of the mutations was confirmed by automated DNA sequencing of selected clones. The PCR products were used to transform JM109 *Escherichia coli* cells. Subsequently, the recombinant plasmids were transferred to BL21(DE3)pLysS *E. coli* , and these clones were used for the screening procedure.

The GO library was screened using a rapid colorimetric assay.[27] Briefly, the colorimetric assay is based on the quantification of hydrogen peroxide produced. Oxidase activity toward 36 mM D-serine, 36 mM D-alanine, or 18 mM glycine was assayed on the crude *E. coli* clones following cell lysis and using HRP and *ortho*-dianisidine (*o*-DNS) assay. The time course of the absorbance change at 450 nm was recorded at room temperature using a microtiter plate reader (Tecan). The average response was calculated, and the clones which outperformed the control were selected for a repetition of the screening. Multiple reparations were performed for the screenings (n = 3 replicates for each substrate). Among the clones showing the highest activity on glycine, six clones were selected for further analyses and biochemical characterization. The DNA of the interesting clones was isolated and sequenced. The Supporting Information contains more details on the experimental methodology corresponding to the screening and clone selection.

Expression and Purification of His-GO WT, H244K, H244F, and H244Q. The pT7(ΔBH) expression plasmids coding for His-tagged wild type, H244K, H244F, and H244Q were transferred to the host BL21(DE3)pLysS *E. coli* strain cells. Recombinant cells were grown under aerobic conditions at 37 °C in LB medium (20 g/L) containing Amp and Cam.[28] Protein expression was induced in the exponential phase (at an OD_{600nm}−2) by adding ITPG to a final concentration of 0.5 mM. The cells were then grown at 30 °C under agitation (130 rpm) and collected after 18 h by centrifugation and stored at −20 °C. Crude extracts were prepared by sonication (four cycles of 30 s each—pulsed and then continuous) of the cell paste suspended with 50 mM disodium pyrophosphate buffer, pH 8.5, containing 5 mM EDTA, 20 μM FAD, 5 mM 2-mercaptoethanol, 0.7 μg/mL pepstatin, and 10 μg/mL deoxyribonuclease I (2−3 mL of buffer/gram of *E. coli* cells). The insoluble fraction of the lysate was removed by centrifugation. The recombinant GO variants were purified from the crude extracts by using a HiTrap chelating affinity chromatography column (GE Healthcare) previously loaded with 100 mM $NiCl_2$ and equilibrated with 50 mM disodium pyrophosphate buffer (pH 7.2), 1 M NaCl, 20 mM imidazole, and 5% glycerol. The purified GOs were then equilibrated with 50 mM disodium pyrophosphate, pH 8.5, and 10% glycerol.[22,26]

The final preparation of GO WT, H244Q, and H244K was stored in 0.01 M phosphate-buffered saline (PBS), pH 7.4, containing 1% glycerol. Enzyme purity was >90% as determined by SDS-PAGE (Figure S1). Enzymes were concentrated with a Centricon ultrafiltration device (MW

https://doi.org/10.1021/acs.analchem.1c03620
Anal. Chem. 2021, 93, 16504−16511

cutoff = 30 kDa, Amicon). Protein concentration of the purified enzymes was determined using the extinction coefficient at 450 nm (11.8 mM^{-1} cm^{-1} for GO and 14.4 mM^{-1} cm^{-1} for GO H244K).[24,26]

GO Activity Assay. Standard polarographic assays (0.253 mM O_2 and 25 °C) for GO WT and GO H244K on 10 or 100 mM glycine in 50 mM sodium pyrophosphate buffer (pH 8.5) were employed.[22,23] One enzyme unit is defined as the amount of enzyme that converts 1 μmol amino acid per minute at 25 °C.[29] Substrate specificity was investigated using a colorimetric assay based on detection of hydrogen peroxide production using a coupled assay with peroxidase and *o*-DNS (ε = 13 mM^{-1} cm^{-1}). Briefly, H_2O_2 produced from GO is reduced by HRP that simultaneously oxidizes *o*-DNS to give a colored compound with an absorption maximum at 440 nm. Different concentrations of standard D-alanine (1 mM), D-serine (1 mM), and glycine (100 μM−10 mM) were used as substrates. The specific activity (SA) for each enzyme on the substrate of interest was calculated as follows

$$\mathrm{SA} = \frac{\Delta \mathrm{Abs}_{440\ \mathrm{nm}}/\mathrm{min}}{\varepsilon_{o\text{-DNS}}} \times \frac{V_{\mathrm{total}}}{v_{\mathrm{enzyme}}} \times [\mathrm{enzyme}] \left(\frac{\mathrm{mg}}{\mathrm{mL}}\right) \quad (1)$$

Electrochemical Experiments. Electrochemical measurements were performed using an electrochemical probe scanner 3 (Heka Elektronik, Lambrecht, Germany; bipotentiostat model PG340). All potentials were recorded relative to a chloridized silver wire (fabricated in-house, radius = 0.125 mm) quasi-reference electrode (Ag/AgCl QRE).[30] All electrochemical solutions were prepared in PBS (0.01 M and pH 7.4). Measurements performed using chronoamperometry, involved a microelectrode (ME) biased at 0.5 V versus Ag/AgCl. All recorded potentials are reported against an Ag/AgCl reference.

GO WT and GO H244K Biosensor Fabrication. For biosensor development, the final GO WT and H244K preparations were concentrated to 50 mg mL^{-1} PBS (pH 7.4) containing 1% glycerol and 25 mg mL^{-1} bovine serum albumin using a Centricon device (MW cutoff = 30 kDa, Amicon). Platinum (Pt) disk MEs (10 μm) were prepared according to a previously reported procedure.[30] Briefly, a soda-lime glass capillary was pulled and a Pt wire was inserted into the capillary, which was then sealed. The ME tip was polished until the Pt wire was exposed, revealing a disk-shaped surface geometry. The final ME was rinsed with deionized water (18.2 MΩ), 70% ethanol, and acetone. The R_g is the ratio of the glass sheath to the diameter of the electroactive surface and was confirmed with optical microscopy using a customized Axio Vert A1 inverted microscope (Zeiss, Oberkochen, Germany) to be between 2 and 3 for all MEs. A permselective polymer was then electrodeposited on the electrode surface using cyclic voltammetry (0 to +1 V, five cycles) with 0.1 M *m*-phenylenediamine (PPD) prepared in 0.01 M PBS (pH 7.4). The full biosensors were fabricated according to a literature protocol.[31] Briefly, 2 μL of each enzyme was drop-cast on a PDMS-coated glass slide. The PPD ME was immersed in the enzymes for five s and then removed to dry for 4 min. This procedure was repeated four times, followed by enzyme cross-linking using glutaraldehyde (50% v/v in H_2O).

Biosensor High-Throughput Assay. Experiments were conducted in a Faraday cage positioned on a vibration dampening table (Micro 60, Halcyonics, Ames, IA, USA) to minimize noise. A custom-made well plate (4 × 5 wells) was fixed to the ELP-3 sample plate (See Supporting Information for information on the well preparation). The biosensor was lowered to approach the well plate using a z-piezo micropositioner until contact was made with the solution in the well (~6 mm). Upon contact with the solution, an electrical connection was made and a chronoamperometric protocol was applied in which a potential of 500 mV was applied at the biosensor tip after a stabilization period of 30 s at 0 V. Following the completion of a 5 min current recording in a single microwell, the biosensor was retracted upward to break the electrical connection, moved 6 mm in the *x*-direction toward the next well, and the approach and recording process was repeated. For each biosensor, independent chronoamperograms were recorded in a 4 × 5 grid. A macros protocol was written to iterate the hopping-mode recording process until recording from all individual wells in each was completed. To move to the next row, the biosensor was moved 4 mm in the y direction. Currents were sampled at 10 Hz.

Glycine Quantification from Astrocytes and Astrocyte-Conditioned Media. All studies using animals were conducted in accordance with the guidelines of the Canadian Council for Animal Care and approved by the Montreal Neurological Institute Animal Care Committee. Primary astrocyte cultures were obtained by mechanically dissociating and discarding non-astrocyte cell types from mixed glial cultures derived from P2 Sprague-Dawley rat pup cortices.[32] Astrocytes were cultured in poly-D-lysine-coated 100 mm dishes in Dulbecco Modified Eagle media (DMEM) containing 10% fetal bovine serum (FBS), penicillin/streptomycin, and L-glutamine and passaged at least three times before use. Cultures were checked with optical microscopy to ensure >95% astrocyte purity. Cells were cultured until confluency, and the media were collected after 7 days and after 10 days for analysis. Astrocyte-conditioned media were passed through 0.22 μm filters and stored at −80 °C until ready for analysis.

Biosensor Application for In Vitro Glycine Detection from Cells. Cultured HEK 293 cells were grown in 100 mm dishes and DMEM (Sigma-Aldrich, Oakville, ON, Canada) supplemented with 9.1% FBS (Thermo Fisher, Ottawa, ON, Canada) and 0.5 mg mL^{-1} primocin (InvivoGen, San Diego, CA, U.S.A.). Following confluency (~7−8 days), the plates were scraped (STEMCELL) and centrifuged for 5 min (6000 rpm) at room temperature to form a cell pellet. The cells were washed with sterile PBS twice and then resuspended in PBS buffer using a pipette tip for buffer exchange. For any biosensor experiment, an aliquot corresponding to 1 × 10^6 cells was transferred to a well on a well plate. The same protocol was repeated for null biosensor measurements and for rat-derived astrocytes.

Data Analysis. All experimental data are presented as the mean of triplicate measurements unless otherwise stated. Error bars represent the standard error of the mean (±SEM). Data were analyzed using in-house-developed software (Sensorlyze), or Python 3.7 and treated in Python 3.7. Electrochemical signals were blank (PBS) signal-corrected, resulting in i_{norm}. To generate the calibration curves, the steady-state signals from the noise-filtered data were extracted at each concentration and fit to a linear regression line. The limit of detection (LOD) corresponds to three times the standard deviation of the blank. The limit of quantification (LOQ) corresponds to 10 times the standard deviation of the blank. Selectivity toward glycine was calculated as follows

https://doi.org/10.1021/acs.analchem.1c03620
Anal. Chem. 2021, 93, 16504−16511

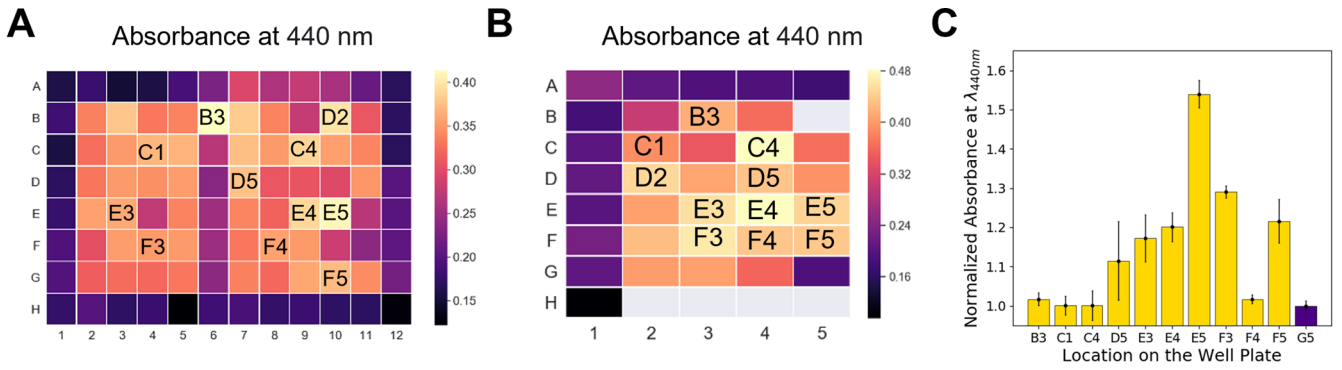

Figure 1. HTS Assay screening results for a GO library at position 244 following 24 h of incubation in 18 mM glycine. (A) Absorbance values (λ = 440 nm) for all GO expressing *E. coli* clones screened in a 96-well plate. Position H11 corresponds to the clone for GO WT, and position H12 corresponds to the control well with no clone present. (B) Absorbance values (440 nm) for GO clones selected from initial screening of 94 clones. Position G5 corresponds to the clone for GO WT, and position H1 corresponds to the control well without *E. coli* cells. Gray boxes represent empty wells. (C) Normalized absorbance values [corrected for the control plate and normalized by a factor of 1 to GO WT (purple, G5)] for the 10 clones (yellow) selected from the screening.

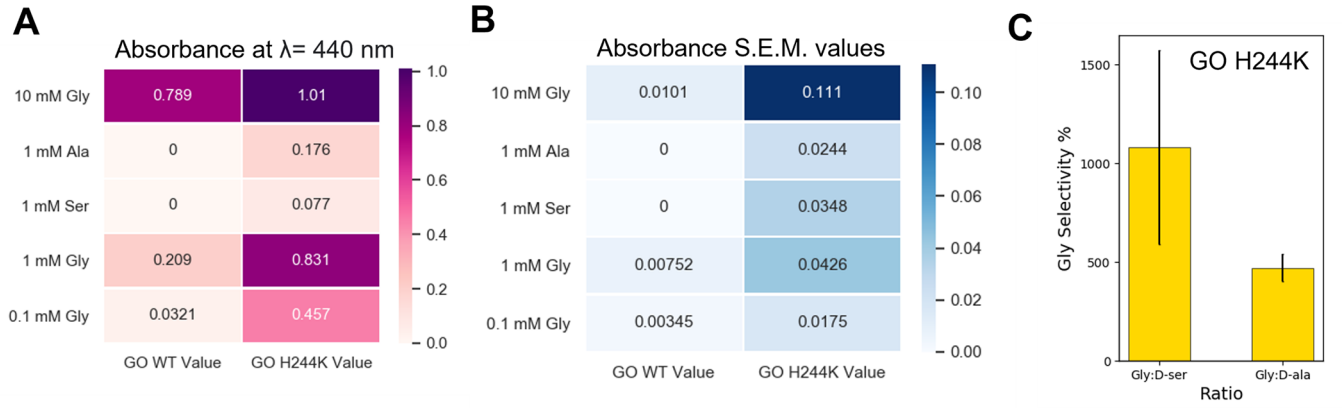

Figure 2. Substrate specificity of GO WT and H244K as determined using spectrophotometric assay (sodium pyrophosphate buffer, pH 8.5). (A) SA (U mg^{-1}) values for the enzymes at various substrate concentrations of D-serine, D-alanine, or glycine. (B) SEM values for the specific activities as reported in panel A. (C) Selectivity of GO H244K enzymes toward glycine over D-serine and D-alanine. Error bars represent mean values ± SEM.

$$\text{selectivity}_{gly} = \left[\frac{SA_{\text{desired product}}}{SA_{\text{undesired product}}}\right] \times 100 = \left[\frac{SA_{gly}}{SA_{\text{D-ser/D-ala}}}\right] \times 100 \quad (2)$$

where SA is the specific activity of the selected amino acid.

RESULTS AND DISCUSSION

Screening for GO Variant Enzymes with High Glycine Activity. Glycine is turned over by GO during the enzyme catalytic cycle, producing H_2O_2 as a byproduct. His-GO WT has a catalytic efficiency of 0.86 s^{-1} mM^{-1}.[26] Enzyme catalytic efficiency, a measure of enzyme specificity and turnover, can be improved through protein engineering.[33−35] To minimize discovery time associated with biocatalyst development with enhanced efficiency for use in biosensor design, we applied a site-saturation mutagenesis approach, namely, mutant library generation and high-throughput activity screening (HTS).

Following the generation of a GO mutant library at the H244 position through site-saturation mutagenesis,[26] a 96-well plate and an automated liquid handling system were used for a colorimetric assay. The signal observed from *o*-DNS assay on 18 mM glycine and the crude extracts of *E. coli* cells expressing GO variants corresponds to the enzyme variant activity.[27] Any alteration in the GO clone activity on glycine was monitored using a change in absorbance at 440 nm (Figure 1A).

After a second round of screenings (Figure 1B), 10 clones with increased glycine activity were identified. To confirm the increased activity of the 10 selected clones, one final screening was performed with only the 10 clones. The absorbance values for these clones normalized to the absorbance for GO WT are presented in Figure 1C. These clones correspond to GO variants with enhanced glycine activity compared to that of GO WT (Figure 1C, gold vs purple), making their use for biosensor development an attractive option.

The most active clones harbored the H244F, H244Q, and H244K substitutions (Figure 1C: E3, E4, and F5). These GO variants expressed their activity on glycine, which was determined using the polarographic method. From the specific activities (Table S1, GO WT: 0.8 U mg^{-1}, GO H244F: 0.523 U mg^{-1}, GO H244K: 1.038 U mg^{-1}, and GO H244Q: 0.177 U mg^{-1}) and literature activities,[26] GO H244K had the highest glycine turnover ratio compared to GO WT (Table S2, 11.22 vs 1.00). As such, the activity of GO WT and H244K was

https://doi.org/10.1021/acs.analchem.1c03620
Anal. Chem. 2021, 93, 16504−16511

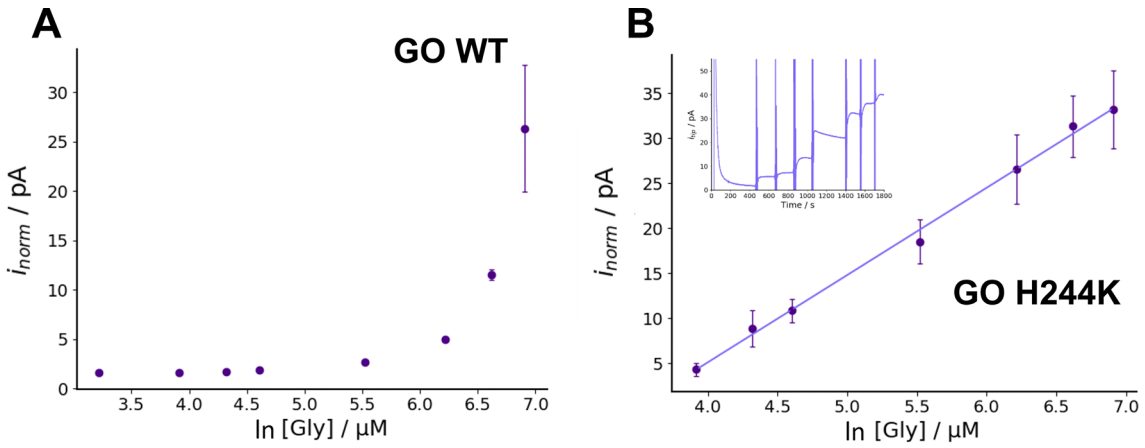

Figure 3. Calibration curves of (A) GO WT and (B) GO H244K-based biosensors in standard solutions of 50,75, 100, 250, 500, 750, and 1000 μM glycine (PBS, pH 7.4). Inset: raw sample current−time curve for different glycine biosensors using GO H244K enzymes. Error bars correspond to the S.E.M (n = 4). LOD = 16.5 ± 2.9 μM and LOQ = 55 ± 4.2 μM.

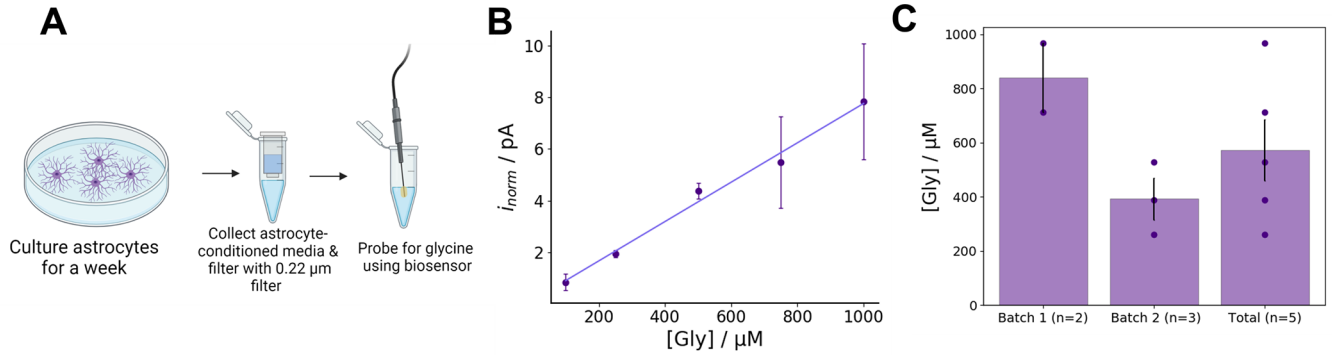

Figure 4. Glycine detection from primary rat cultured astrocytes using GO H244K biosensors. (A) Schematic of the experimental protocol. (B) Biosensor calibration curve in standard glycine solutions prepared in DMEM. (C) Concentrations obtained from biosensor calibrations for individual batches and for the batches combined. Batch 1 corresponds to media collected after 7 days. Batch 2 corresponds to media collected after 10 days; total corresponds to the average of all batches. Average concentrations ± SEM are shown.

determined at different glycine concentrations using spectrophotometric *o*-DNS assays (Figure 2). At all tested concentrations (0.1, 1, and 10 mM), GO H244K had higher glycine activity than GO WT. Moreover, GO H244K had high activity toward glycine compared to D-serine and D-alanine (Figure 2C), two amino acids of neurological relevance which are simultaneously present in the central nervous system.[36−38]

Assessing the Performance of GO WT and H244K Biosensors. Using both GO WT and H244K, the enzymes were incorporated into biosensors. Through enzyme immobilization on PPD-Pt MEs, biosensors were fabricated and calibrated in standard solutions of glycine.[39] To rapidly generate calibration curves, Sensorlyze, an in-house python-based software tool developed by the author, was used for biosensor performance assessment. Sensorlyze software automates data processing and manipulation by converting raw data files into figures and allows users to generate calibration curves from multiple data files and provides statistics such as linear regression parameters and limits of detection and quantification. Sensorlyze was also used to extract steady-state currents from multiple chronoamperograms and to average these values over a 30 s range.

The current response of GO WT and GO H244K was linearly related to the logarithmic value of the glycine concentration within the range of 50−1000 μM (Figure 3). GO WT at 13.3 mg mL^{-1} resulted in calibration curves with lower sensitivity (Figure S3A) compared to the more concentrated GO WT at 50 mg mL^{-1} (Figure S3B). Additionally, the non-log calibration curves for GO WT and GO H244K were non-linear and are presented in Figure S3.

To assess the stability of the biosensors, GO H244K and GO WT biosensors were stored at 4 and −20 °C following an initial calibration. Both biosensors lost sensitivity following 2 week storage at −20 °C (Figure S4A,B). The lack of response was due to enzyme film delamination, suggesting that the adsorption of GO requires improvement for increased biosensor lifetime. GO biosensors were stored dry at 4 °C and calibrated the following day. A linear calibration curve was obtained for GO H244K (Figure S4C).

GO H244K Biosensors Detect Glycine in Astrocyte-Conditioned Media. Astrocytes are thought to be a major source of glycine[40] and were studied with GO H244K biosensors (Figure 4A). The biosensor was first calibrated in standard solutions of glycine spiked into DMEM buffer, which already contained 400 μM glycine (Figure 4B). Following astrocyte culture, media collection and filtering, and biosensor calibration, the biosensor was applied for glycine detection in 300 μL of filtered, astrocyte-conditioned DMEM. Media from two sets of cultures were collected. From batch 1, the media were collected after 7 days of conditioning. From batch 2, the

https://doi.org/10.1021/acs.analchem.1c03620
Anal. Chem. 2021, 93, 16504−16511

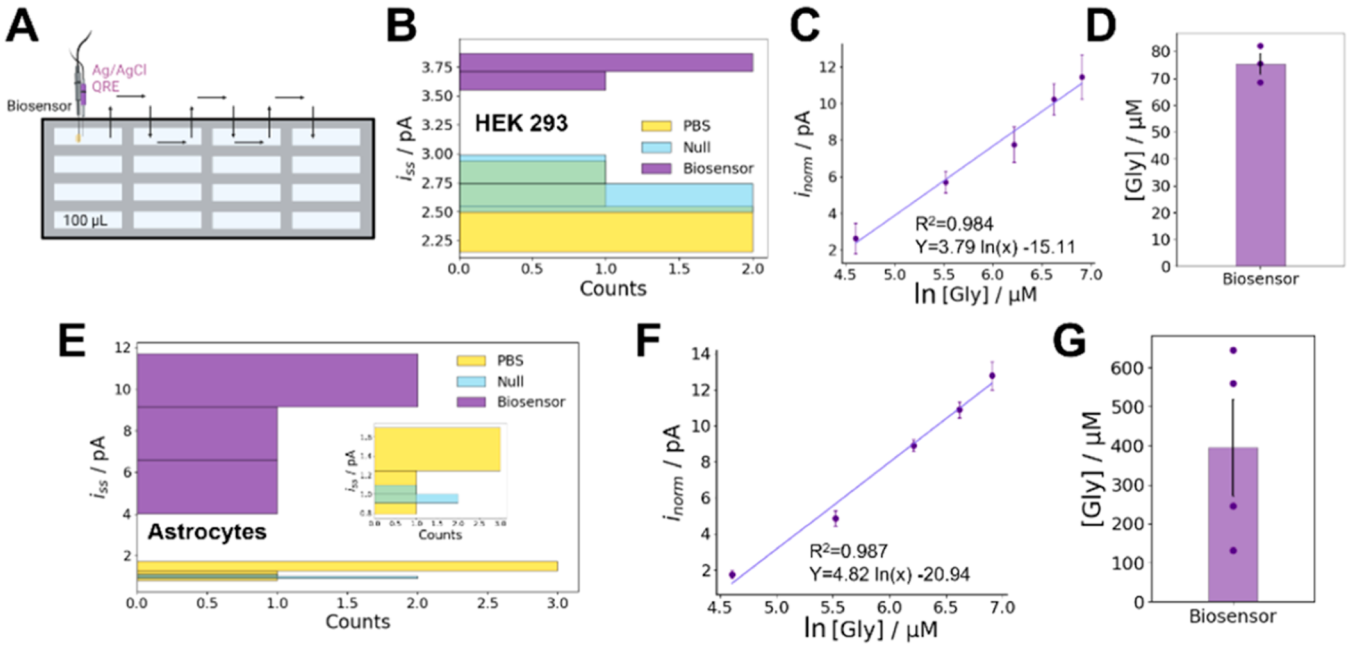

Figure 5. High-throughput hopping-mode real-time glycine detection from multiple biological analytes. (A) Schematic of the electrochemical experimental setup. (B) Buffer-normalized currents from HEK 293 cells using the null and enzymatic biosensors. (C) Calibration curve with the GO H244K enzymatic biosensors. (D) Corresponding current reading from HEK 293 cells using the biosensor. The average reading corresponds to 75.4 ± 3.91 μM. (E) Histogram of the steady-state currents from null and active biosensors immersed in buffer and astrocytes. (F) Calibration curve of the biosensor prior to glycine detection from astrocytes; corresponding current readings of glycine released from astrocytes following a 30 min biosensor incubation period. (G) Average reading corresponds to 395.7 ± 123 μM. Error bars correspond to ±SEM.

media were collected after 10 days of conditioning. Using the biosensor, an average of 572 ± 113 μM glycine was measured (Figure 4C), suggesting batch-to-batch differences. Although DMEM has 400 μM glycine, it was possible to measure additional glycine levels as shown in Figure 4. From the biosensor readings in Figure 4, it is suggested that astrocytes do release glycine, possibly through astrocyte glycine transporters, as shown in the published literature.[40−43]

Achieving Glycine Detection from Live HEK 293 Cells and Astrocytes. Microelectrode biosensors are particularly useful for localized quantification of analytes. To assess the performance of these biosensors in glycine release measurements using an automated methodology, a custom-made micro-sized well plate was prepared as discussed in the Experimental Section. In combination with a 0.125 mm Ag/AgCl quasi reference electrode, the biosensor was approached to the solution on the microwell plate using a z-piezo motor. A constant voltage of 0.5 V was applied at the biosensor tip and when the biosensor was immersed in solution, a faradaic current corresponding to the oxidation of H_2O_2 was recorded. The biosensor was moved from one well to another using a hopping mode with an ELP motor system, and the current from each sample was recorded (Figure 5A). To evaluate glycine release, the biosensor was immersed in 100 μL of HEK 293 cell-conditioned medium (1×10^6 cells in PBS buffer), which was pipetted into one of the wells on the well plate. The current from the HEK 293 cells was monitored over a period of 30 min, and the steady-state current after 30 min was extracted from chronoamperograms (Figure 5B purple, Figure S5) and compared against the background signal from the biosensor in PBS buffer (Figure 5B yellow). The same protocol was repeated using a null biosensor (Figure 5B blue). The biosensor calibration curve (Figure 5C) was then used to convert the current responses of the biosensor from the HEK 293 cell-conditioned medium into glycine concentrations (Figure 5D). Similarly, glycine release from astrocytes was monitored using the active and null biosensors (Figure 5E purple vs blue), and the signal was compared against the biosensor response in PBS buffer (Figure 5E, yellow). The biosensor calibration curve (Figure 5F) was then used to convert the current responses of the biosensor to astrocyte-conditioned medium into glycine concentrations (Figure 5G). The concentrations recorded from Figure 5D and G demonstrate that GO H244K biosensors are useful tools for real-time glycine detection from multiple cell types. Moreover, Figure 5 shows that astrocytes release significantly larger amounts of glycine (395.7 ± 123 μM, Figure 5D) compared to HEK 293 cells (75.4 ± 3.91 μM, Figure 5G). Astrocytes demonstrate ~fivefold greater release of glycine than HEK 293 cells. The relatively higher astrocytic glycine release is consistent with the literature, suggesting that astrocytes store glycine and that glycine release is mediated through the Asc-1 transporter, which is not typically found in HEK 293 cells.[40−43] Moreover, liquid chromatography−mass spectrometry (LC−MS) experiments demonstrate the presence of glycine in these cell samples, confirming the release of glycine through both biosensor and LC−MS measurements (Figure S6). Finally, the potential of using Triton X-100 and Tween-20 to lyse cells for release of stored glycine is also presented in Figure S7. The effect of the surfactants on the biosensor response is shown to be negligible.

CONCLUSIONS

In this work, we demonstrated the first enzymatic amperometric biosensor fabricated and applied for glycine detection from cells based on GO H244K. Mutagenesis and high-throughput enzyme screening enabled the rapid discovery of enzyme variants with enhanced glycine turnover activity. The

https://doi.org/10.1021/acs.analchem.1c03620
Anal. Chem. 2021, 93, 16504−16511

performance of the GO H244K biosensor superseded that of the GO WT biosensor, and the GO H244K biosensor demonstrated high reproducibility. Using only 100 μL of cells, glycine was detected from both HEK 293 cells and astrocytes without the need for additional reagents. Although these sensors were shown to be applicable for detection of glycine, future work entails quantification of glycine concentration changes in real time at different time points. Additionally, sensitivity improvements of such biosensors occurs possibly through increasing the microelectrode backbone surface roughness or the generation of a double- or triple-variant enzyme with even further enhanced glycine selectivity. Given this paper's advancements in reducing enzyme discovery times, biosensor optimization, and assay miniaturization and automation, this system can be developed with minimal effort potentially for any stable oxidase enzyme, thus extending the range of analytes probed with such sensors. These sensors may then be used to study glycinergic functions and mechanisms in the brain or as clinical tools for glycine analysis.

■ ASSOCIATED CONTENT

Supporting Information

The Supporting Information is available free of charge at https://pubs.acs.org/doi/10.1021/acs.analchem.1c03620.

Detailed experimental methods and supporting figures on supporting results (PDF)

■ AUTHOR INFORMATION

Corresponding Author

Janine Mauzeroll − *Department of Chemistry, McGill University, Montreal, Quebec H3A 0B8, Canada;* orcid.org/0000-0003-4752-7507; Phone: 514-398-3898; Email: Janine.mauzeroll@mcgill.ca

Authors

Siba Moussa − *Department of Chemistry, McGill University, Montreal, Quebec H3A 0B8, Canada;* orcid.org/0000-0002-6873-2019

Elena Rosini − *Dipartimento di Biotecnologie e Scienze della Vita, Università degli studi deII'Insubria, Varese 21100, Italy;* orcid.org/0000-0001-8384-7992

Daryan Chitsaz − *Integrated Program in Neuroscience, McGill University, Montreal, Quebec H3A 1A1, Canada*

Loredano Pollegioni − *Dipartimento di Biotecnologie e Scienze della Vita, Università degli studi deII'Insubria, Varese 21100, Italy;* orcid.org/0000-0003-1733-7243

Timothy E. Kennedy − *McGill Program in Neuroengineering, Department of Neurology and Neurosurgery, Montreal Neurological Institute, McGill University, Montreal, Quebec H3A 2B4, Canada;* orcid.org/0000-0003-4454-5080

Complete contact information is available at: https://pubs.acs.org/10.1021/acs.analchem.1c03620

Author Contributions

All authors have given approval to the final version of the article.

Notes

The authors declare no competing financial interest.

■ ACKNOWLEDGMENTS

This work was supported by the NSERC and MITACS. Part of this work was carried out by S.M. during a 3 month period at the University of Insubria. E.R. and L.P. thank the support from FAR Fond di Ateneo per la Ricerca.

■ REFERENCES

(1) Moussa, S.; Mauzeroll, J. *J. Electrochem. Soc.* **2019**, *166*, G25.
(2) Newman, J. D.; Turner, A. P. F. *Biosens. Bioelectron.* **2005**, *20*, 2435−2453.
(3) Chen, C.; Xie, Q.; Yang, D.; Xiao, H.; Fu, Y.; Tan, Y.; Yao, S. *RSC Adv.* **2013**, *3*, 4473−4491.
(4) Moussa, S.; Van Horn, M. R.; Shah, A.; Pollegioni, L.; Thibodeaux, C. J.; Ruthazer, E. S.; Mauzeroll, J. *J. Electrochem. Soc.* **2021**, *168*, 025502.
(5) Polcari, D.; Kwan, A.; Van Horn, M. R.; Danis, L.; Pollegioni, L.; Ruthazer, E. S.; Mauzeroll, J. *Anal. Chem.* **2014**, *86*, 3501−3507.
(6) MacKay, M.-A. B.; Kravtsenyuk, M.; Thomas, R.; Mitchell, N. D.; Dursun, S. M.; Baker, G. B. *Front. Psychiatr.* **2019**, *10*, 25.
(7) Isoaho, N.; Peltola, E.; Sainio, S.; Wester, N.; Protopopova, V.; Wilson, B. P.; Koskinen, J.; Laurila, T. *J. Phys. Chem. C* **2017**, *121*, 4618−4626.
(8) Qiu, Q.-F.; Zhang, F.-L.; Tang, Y.; Zhang, X.-W.; Jiang, H.; Liu, Y.-L.; Huang, W.-H. *Electroanalysis* **2018**, *30*, 1054−1059.
(9) Njagi, J.; Chernov, M. M.; Leiter, J. C.; Andreescu, S. *Anal. Chem.* **2010**, *82*, 989−996.
(10) Moreira, F. T. C.; Sale, M. G. F.; Di Lorenzo, M. *Biosens. Bioelectron.* **2017**, *87*, 607−614.
(11) Zhang, W. H.; Herde, M. K.; Mitchell, J. A.; Whitfield, J. H.; Wulff, A. B.; Vongsouthi, V.; Sanchez-Romero, I.; Gulakova, P. E.; Minge, D.; Breithausen, B.; Schoch, S.; Janovjak, H.; Jackson, C. J.; Henneberger, C. *Nat. Chem. Biol.* **2018**, *14*, 861−869.
(12) Harsing, L. G.; Matyus, P. *Brain Res. Bull.* **2013**, *93*, 110−119.
(13) Wang, W.; Wu, Z.; Dai, Z.; Yang, Y.; Wang, J.; Wu, G. *Amino Acids* **2013**, *45*, 463−477.
(14) Weinberg, J. M.; Bienholz, A.; Venkatachalam, M. A. *Cell. Mol. Life Sci.* **2016**, *73*, 2285−2308.
(15) Razak, M. A.; Begum, P. S.; Viswanath, B.; Rajagopal, S. *Oxid. Med. Cell. Longevity* **2017**, *2017*, 1−8.
(16) Voehringer, P.; Fuertig, R.; Ferger, B. *J. Chromatogr. B: Anal. Technol. Biomed. Life Sci.* **2013**, *939*, 92−97.
(17) Forgacsova, A.; Galba, J.; Mojzisova, J.; Mikus, P.; Piestansky, J.; Kovac, A. *J. Pharm. Biomed. Anal.* **2019**, *164*, 442−451.
(18) Pérez-Ràfols, C.; Liu, Y.; Wang, Q.; Cuartero, M.; Crespo, G. A. *Sensors* **2020**, *20*, 4049.
(19) Vidotti, M.; de Torresi, S. I. C.; Kubota, L. T. *Sens. Actuators, B* **2008**, *135*, 245−249.
(20) Roushani, M.; Shamsipur, M.; Pourmortazavi, S. M. *J. Appl. Electrochem.* **2012**, *42*, 1005−1011.
(21) Manjunatha, J. G. G. *J. Food Drug Anal.* **2018**, *26*, 292−299.
(22) Molla, G.; Motteran, L.; Job, V.; Pilone, M. S.; Pollegioni, L. *Eur. J. Biochem.* **2003**, *270*, 1474−1482.
(23) Job, V.; Marcone, G. L.; Pilone, M. S.; Pollegioni, L. *J. Biol. Chem.* **2002**, *277*, 6985−6993.
(24) Boselli, A.; Rosini, E.; Marcone, G. L.; Sacchi, S.; Motteran, L.; Pilone, M. S.; Pollegioni, L.; Molla, G. *Biochimie* **2007**, *89*, 1372−1380.
(25) Mörtl, M.; Diederichs, K.; Welte, W.; Molla, G.; Motteran, L.; Andriolo, G.; Pilone, M. S.; Pollegioni, L. *J. Biol. Chem.* **2004**, *279*, 29718−29727.
(26) Rosini, E.; Piubelli, L.; Molla, G.; Frattini, L.; Valentino, M.; Varriale, A.; D'Auria, S.; Pollegioni, L.; Rosini, C. E. *FEBS J.* **2014**, *281*, 3460.
(27) Rosini, E.; Caldinelli, L.; Piubelli, L. *Front. Mol. Biosci.* **2018**, *4*, 102.
(28) Job, V.; Molla, G.; Pilone, M. S.; Pollegeoni, L. *Eur. J. Biochem.* **2002**, *269*, 1456−1463.
(29) Sacchi, S.; Lorenzi, S.; Molla, G.; Pilone, M. S.; Rossetti, C.; Pollegioni, L. *J. Biol. Chem.* **2002**, *277*, 27510−27516.
(30) Danis, L.; Polcari, D.; Kwan, A.; Gateman, S. M.; Mauzeroll, J. *Anal. Chem.* **2015**, *87*, 2565−2569.

(31) Polcari, D.; Perry, S. C.; Pollegioni, L.; Geissler, M.; Mauzeroll, J. *ChemElectroChem* **2017**, *4*, 920−926.
(32) McCarthy, K. D.; de Vellis, J. *J. Cell Biol.* **1980**, *85*, 890−902.
(33) Duan, X.; Chen, J.; Wu, J. *Appl. Environ. Microbiol.* **2013**, *79*, 4072−4077.
(34) Jaouadi, B.; Aghajari, N.; Haser, R.; Bejar, S. *Biochimie* **2010**, *92*, 360−369.
(35) Molloy, S.; Nikodinovic-Runic, J.; Martin, L. B.; Hartmann, H.; Solano, F.; Decker, H.; O'Connor, K. E. *Biotechnol. Bioeng.* **2013**, *110*, 1849−1857.
(36) Mothet, J. P.; Billard, J. M.; Pollegioni, L.; Coyle, J. T.; Sweedler, J. V. *Acta Physiol.* **2019**, *226*, No. e13257.
(37) Murtas, G.; Sacchi, S.; Valentino, M.; Pollegioni, L. *Front. Mol. Biosci.* **2017**, *4*, 88.
(38) Le Bail, M.; Martineau, M.; Sacchi, S.; Yatsenko, N.; Radzishevsky, I.; Conrod, S.; Ait Ouares, K.; Wolosker, H.; Pollegioni, L.; Billard, J.-M.; Mothet, J.-P.; Snyder, S. H. *Proc. Natl. Acad. Sci. U.S.A.* **2015**, *112*, E204−E213.
(39) Moussa, S.; Murtas, G.; Pollegioni, L.; Mauzeroll, J. *ACS Appl. Bio Mater.* **2021**, *4*, 5598−5604.
(40) Shibasaki, K.; Hosoi, N.; Kaneko, R.; Tominaga, M.; Yamada, K. *J. Neurochem.* **2017**, *140*, 395−403.
(41) Holopainen, I.; Kontro, P. *J. Neurosci. Res.* **1989**, *24*, 374−383.
(42) Rosenberg, D.; Artoul, S.; Segal, A. C.; Kolodney, G.; Radzishevsky, I.; Dikopoltsev, E.; Foltyn, V. N.; Inoue, R.; Mori, H.; Billard, J.-M.; Wolosker, H. *J. Neurosci.* **2013**, *33*, 3533.
(43) Hogerton, A. L.; Bowser, M. T. *Anal. Chem.* **2013**, *85*, 9070−9077.

NOTE ADDED AFTER ASAP PUBLICATION

This paper was published ASAP on November 29, 2021, with a spelling error in an author's name. The corrected version was reposted on November 30, 2021.

https://doi.org/10.1021/acs.analchem.1c03620
Anal. Chem. 2021, 93, 16504−16511